ACS APPLIED MATERIALS & INTERFACES

Research Article

www.acsami.org

Efficient Polymer Solar Cells Based on Poly(3-hexylthiophene) and Indene–C_{60} Bisadduct Fabricated with Non-halogenated Solvents

Xia Guo,[†,‡] Maojie Zhang,*[,†] Chaohua Cui,[†] Jianhui Hou,*[,†] and Yongfang Li*[,†,§]

[†]Beijing National Laboratory for Molecular Sciences, Institute of Chemistry, Chinese Academy of Sciences, Beijing 100190, People's Republic of China

[‡]University of Chinese Academy of Sciences, Beijing 100049, People's Republic of China

[§]College of Chemistry, Chemical Engineering and Materials Science, Soochow University, Suzhou, Jiangsu 215123, People's Republic of China

Supporting Information

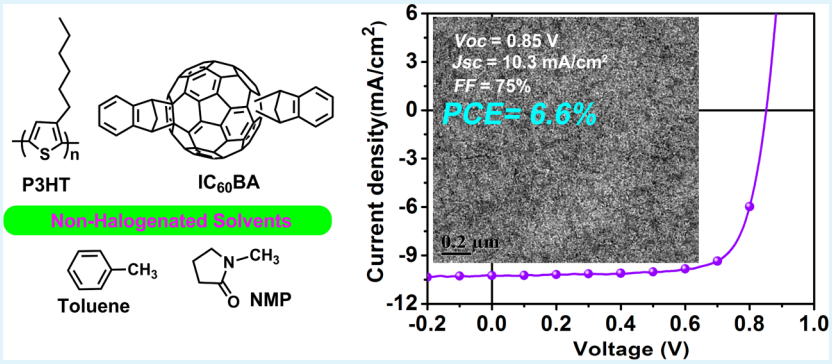

ABSTRACT: The photovoltaic performance of poly(3-hexylthiophene) (P3HT) has been improved greatly by using indene–C_{60} bisadduct (ICBA) as acceptor instead of phenyl-C_{61}-butyric acid methyl ester (PCBM). However, the solvent of dichlorobenzene (DCB) used in fabricating polymer solar cells (PSCs) limited the application of the PSCs, because of the environmental problem caused by the harmful halogenated solvent. In this work, we fabricated the PSCs based on P3HT/ICBA processed with four low-harmful non-halogenated solvents of toluene, *o*-xylene, *m*-xylene, and *p*-xylene. The PSCs based on P3HT/ICBA (1:1, w/w) with toluene as the solvent exhibit the optimized power conversion efficiency (PCE) of 4.5% with open-circuit voltage (V_{oc}) of 0.84 V, short circuit current density (J_{sc}) of 7.2 mA/cm^2, and fill factor (FF) of 71%, under the illumination of AM 1.5G at 100 mW/cm^2. Upon using 1% *N*-methyl pyrrolidone (NMP) as a solvent additive in the toluene solvent, the PCE of the PSCs was greatly improved to 6.6% with a higher J_{sc} of 10.3 mA/cm^2 and a high FF of 75%, which is even higher than that of the devices fabricated with halogenated DCB solvent. The X-ray diffraction (XRD) measurement shows that the crystallinity of P3HT increased with the NMP additive. The investigations on morphology of the active layers by atomic force microscopy (AFM) and transmission electron microscopy (TEM) indicate that the NMP additive promotes effective phase separation and formation of nanoscaled interpenetrating network structure of the active layer, which is beneficial to the improvement of J_{sc} and PCE for the PSCs fabricated with toluene as the solvent.

KEYWORDS: *polymer solar cells, non-halogenated solvents, indene–C_{60} bisadduct, toluene solvent, N-methyl pyrrolidone additive*

INTRODUCTION

Bulk-heterojunction (BHJ) polymer solar cells (PSCs) possess a simple sandwich structure with a thin blend layer of a conjugated polymer donor and a fullerene derivative acceptor between two electrodes. The two electrodes include a high workfunction positive electrode and a low workfunction negative electrode, and at least one of them should be transparent. In comparison to inorganic semiconductor solar cells, PSCs demonstrate advantages of low cost, lightweight, and capability to be fabricated into flexible devices. Therefore, in recent years, PSCs have drawn great interest from basic research scientists and the industrial community.[1−11]

Poly(3-hexylthiophene) (P3HT) is the most representative conjugated polymer donor, with the advantages of higher hole mobility and crystalline structure, which makes it easy to form a nanoscaled interpenetrating network with fullerene derivative acceptors. In addition, good reproducibility of the photovoltaic performance and thicker (ca. 200 nm) optimized active-layer thickness of the PSCs based on P3HT as a donor are also very attractive for large area production of the PSCs. Therefore, a large amount of research work has focused on the optimization

Received: February 10, 2014
Accepted: May 9, 2014
Published: May 9, 2014

   dx.doi.org/10.1021/am500836u | ACS Appl. Mater. Interfaces 2014, 6, 8190–8198

Scheme 1. Molecular Structures of (a) Active-Layer Materials and (b) Non-halogenated Solvents

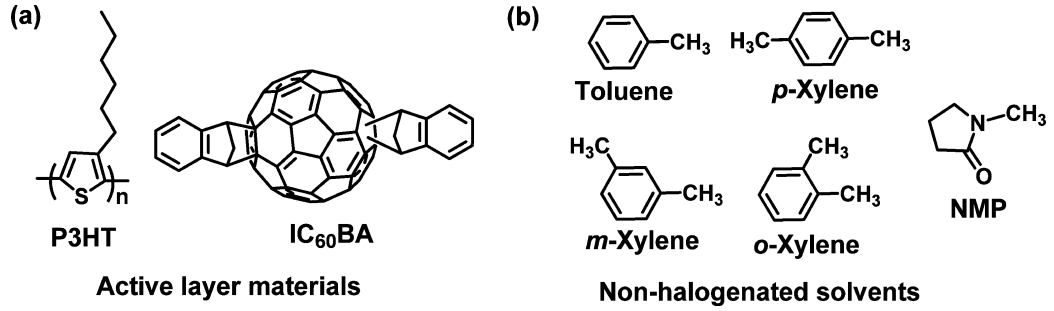

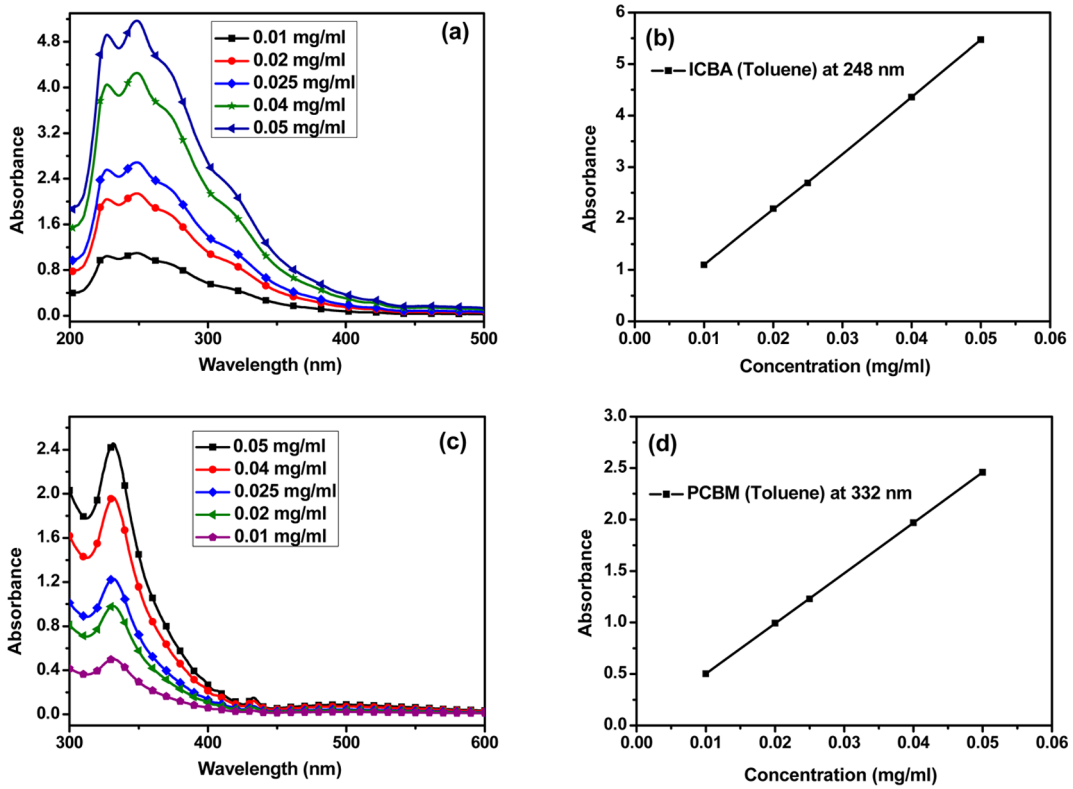

Figure 1. Absorption spectra for calculating solubility: (a and c) absorption spectra of standard solutions of ICBA and PCBM, respectively, (b) plot of ICBA absorbance at 248 nm versus concentration, and (d) plot of PCBM absorbance at 332 nm versus concentration.

of the photovoltaic performance of P3HT by thermal annealing,[12] solvent annealing,[13] and new acceptors.[14−28] Especially, the fullerene bisadduct acceptors with higher lowest unoccupied molecular orbital (LUMO) energy level than $PC_{60}BM$ ([6,6]-phenyl-C_{61}-butyric acid methyl ester) improved the photovoltaic performance of P3HT greatly.[16−25] For example, with indene−C_{60} bisadduct (ICBA) as an acceptor and *o*-dichlorobenzene (*o*-DCB) as a processing solvent, the open circuit voltage (V_{oc}) and power conversion efficiency (PCE) of the PSCs based on P3HT reached 0.84 V and 6.48%, respectively,[18] in comparison to the open-circuit voltage (V_{oc}) of 0.58 V and PCE of 3.84% for the PSCs with phenyl-C_{61}-butyric acid methyl ester (PCBM) as an acceptor under the same experimental conditions. However, the halogenated solvent of *o*-DCB is toxic, which is a serious problem for future large area fabrication and application, because the solvent has to be evaporated to air during the device fabrication processes. Actually, the solvents used at present in fabricating high-performance PSCs are all of the toxic halogenated solvents, including chloroform (CF), chlorobenzene (CB), and *o*-DCB. Therefore, it is of crucial importance to replace the toxic halogenated solvents with environmentally friendly solvent.

Non-halogenated organic solvents, such as toluene and isomers of xylene, are of low toxicity and easier to be removed from their environmental accumulation.[29] Actually, toluene and xylene are widely used solvents in fabricating polymer light-emitting diodes (PLEDs) because they are good solvents for the representative light-emitting polymers of poly(2-methoxy-5-[20-ethyl-hexyloxy]-1,4-phenylenevinylene) (MEH-PPV) and poly(2-methoxy-5-(30,70-dimethyloctyloxy)-1,4-phenylenevinylene) (MDMO-PPV). However, in early studies of PSCs based on MEH-PPV or MDMO-PPV as the donor and $PC_{60}BM$ as the acceptor, the devices fabricated with *o*-DCB as the solvent showed better photovoltaic performance than that processed with xylene,[30] and the CB solvent demonstrated 2.6 times higher efficiency than the toluene solvent for the PSCs based on MDMO-PPV/PCBM.[31] Then, in the following

dx.doi.org/10.1021/am500836u | ACS Appl. Mater. Interfaces 2014, 6, 8190−8198

studies of PSCs, almost all of the researchers used CB, *o*-DCB, or CF as the solvents to fabricate the devices for pursuing higher efficiency. Recently, non-halogenated solvents attracted attention from the consideration of environmental issues caused by the halogenated solvents.[32−35] Park et al. used a mixed solvent of acetophenone and mesitylene instead of *o*-DCB in fabricating the PSCs based on P3HT/PCBM and obtained a PCE of 3.38%.[32] Jen et al. reported high-efficiency PSCs based on poly(indacenodithiophene-*co*-phenanthro[9,10-*b*]quinoxaline) (PIDT-PhanQ) with PCE > 6% using toluene as the processing solvent and 2% 1-methylnaphthalene as the solvent additive[33] and PCE > 7% for the PSCs based on indacenodithieno[3,2-*b*]thiophene−difluorobenzothiadiazole (PIDTT−DFBT) using 1,2,4-trimethylbenzene as the processing solvent and 2.5 vol % of 1,2-dimethylnaphthalene as the solvent additive.[34]

In this work, we used the non-halogenated solvent, including toluene, *o*-xylene, *m*-xylene, and *p*-xylene (as shown in Scheme 1), to fabricate the PSCs based on P3HT/ICBA and optimized the photovoltaic performance of the PSCs using non-halogenated *N*-methyl pyrrolidone (NMP) solvent additive. Under the optimized conditions with the P3HT/ICBA weight ratio of 1:1, using toluene solvent with 1% vol NMP additive and pre-thermal annealing at 150 °C for 10 min, a PCE as high as 6.6% was achieved, with a V_{oc} of 0.85 V, a short circuit current density (J_{sc}) of 10.3 mA/cm^2, and a fill factor (FF) of 75%, under the illumination of AM 1.5G, 100 mW/cm^2. The photovoltaic performance of the PSCs processed with the non-halogenated solvent is even better than that of the device processed with the halogenated *o*-DCB solvent.

RESULTS AND DISCUSSION

Photovoltaic Properties. First, we fabricated the P3HT/PCBM-based PSC devices using non-halogenated toluene solvent with a typical structure of indium tin oxide (ITO)/poly(3,4-ethylenedioxythiophene):poly(styrene sulfonate) (PEDOT:PSS)/P3HT/PCBM/Ca/Al. Figure S1 of the Supporting Information shows the current density−voltage (*J*−*V*) and the external quantum efficiency (EQE) curves of the PSCs based on P3HT/PCBM (1:1, w/w) using toluene as the solvent under the optimized conditions of P3HT/PCBM weight ratio of 1:1 and pre-thermal annealing at 150 °C for 10 min. The V_{oc}, J_{sc}, and FF of the PSC are 0.64 V, 5.0 mA/cm^2, and 58%, respectively, leading to a low PCE of 1.8%.

As known, the solubility of a fullerene derivative strongly affects the efficiency of the PSCs,[36] PCBM shows poor solubility in many non-halogen solvents,[37] but ICBA shows good solubility in the non-halogenated solvent;[38] therefore, we can expect that the PSCs based on P3HT/ICBA with non-halogenated solvent could obtain a higher PCE. To understand the effect of solubility of the fullerene derivatives in the non-halogenated solvent on the photovoltaic performance of the PSCs processed with the non-halogenated solvent, we measured the solubility of ICBA and PCBM in the toluene solvent with the standard calibration curve method. The detailed measurement processes are described in the Experimental Section. Figure 1 shows the standard calibration curves for ICBA and PCBM. The solubility values calculated from the working curves are 94.5 mg/mL for ICBA and 9.5 mg/mL for PCBM. Obviously, ICBA is a promising acceptor for the PSCs processed with toluene solvent from the solubility point of view.

The PSC devices were fabricated with a typical structure using P3HT/ICBA (1:1, w/w) as the active layer with pre-thermal annealing at 150 °C for 10 min, to investigate the effect of processing solvents (*o*-DCB, toluene, *o*-xylene, *m*-xylene, and *p*-xylene) on the photovoltaic performance of the PSCs. Figure 2a shows the dark and photo *J*−*V* curves of the optimized PSCs

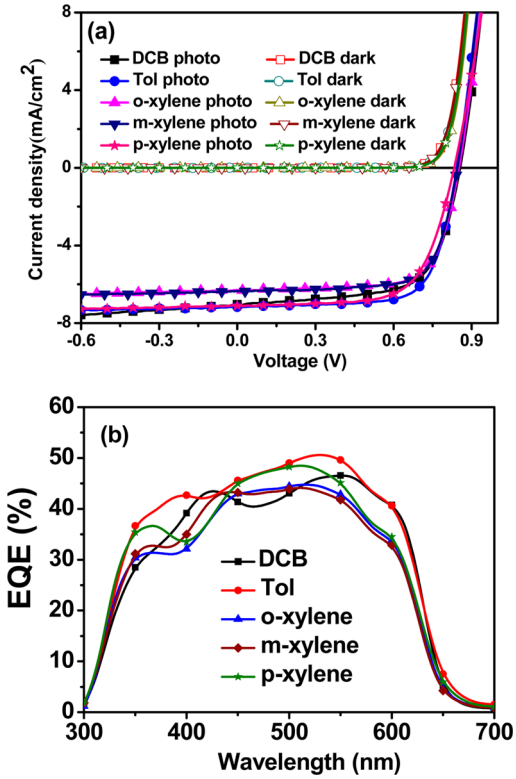

Figure 2. (a) *J*−*V* curves of the polymer solar cells based on P3HT/ICBA (1:1 w/w) fabricated with different solvents. (b) EQE curves of the corresponding devices.

based on P3HT/ICBA with different processing solvents. Table 1 summarizes the photovoltaic performance data of the PSCs, including the V_{oc}, J_{sc}, FF, and PCE of the devices. It can be seen that, when the processing solvent is the commonly used *o*-DCB, the PCE is 4.0%. The non-halogenated solvent toluene gave better photovoltaic performance with PCE of 4.5%, while the non-halogenated solvents of *o*-xylene, *m*-xylene, and *p*-xylene gave similar PCE values of 3.9−4.0% in comparison to the halogenated solvent *o*-DCB. Obviously, the PSCs fabricated with the toluene solvent demonstrated the highest PCE with a higher J_{sc} and a higher FF. Furthermore, the morphologies of the P3HT/ICBA blend coated from different non-halogenated solvent were investigated by atomic force microscopy (AFM), as shown in Figure S2 of the Supporting Information. It was found that the blend film coated from toluene showed the best morphology with well phase separation, which is in agreement with the device performance.

The EQE of the PSCs based on P3HT/ICBA (1:1, w/w) with different processing solvents are shown in Figure 2b. The J_{sc} values integrated from EQE spectra (as shown in Table 1) agree very well with those measured from the corresponding PSCs mentioned above. Processed from different solvents, the EQE curves of the PSCs cover a broad wavelength range from 350 to 650 nm, and the device fabricated with toluene solvent displayed an EQE up to 50%, which is higher than that of the

Table 1. Photovoltaic Performance Data of the PSCs Based on P3HT/ICBA (1:1, w/w) Processed with Different Solvents under the Illumination of AM 1.5G, 100 mW/cm^2

processing solvent	V_{oc} (V)	J_{sc}[a] (mA/cm^2)	FF (%)	PCE best (%)	PCE average[b] (%)	thickness (nm)
o-DCB	0.86 ± 0.03	7.0 ± 0.2 (6.9)	66 ± 1	4.0	3.8	205 ± 5
toluene	0.84 ± 0.03	7.2 ± 0.2 (7.2)	71 ± 1	4.5	4.4	300 ± 5
o-xylene	0.85 ± 0.03	6.3 ± 0.2 (6.3)	72 ± 1	3.9	3.8	210 ± 5
m-xylene	0.85 ± 0.03	6.4 ± 0.2 (6.3)	71 ± 1	3.9	3.8	210 ± 5
p-xylene	0.83 ± 0.03	7.1 ± 0.2 (7.0)	67 ± 1	4.0	3.8	220 ± 5

[a]The values in parentheses are the J_{sc} values calculated from EQE spectra. [b]The average PCE obtained from 20 devices.

devices fabricated with the solvent of *o*-DCB, *o*-xylene, or *m*-xylene. It should be mentioned that the optimized active-layer thickness of the PSCs with the toluene solvent is ca. 300 nm, which is thicker than the devices fabricated with other solvents. The thicker active-layer thickness of the PSCs with the toluene solvent is another advantage of the toluene solvent, because the thicker active-layer thickness will make the fabrication of large area devices easier and will be beneficial for future application of the PSCs.

Because of the best performance of toluene among the four non-halogenated solvents in fabricating the PSCs, we used the solvent additive[39,40] to further optimize the photovoltaic performance of the PSCs with toluene as the processing solvent. In considering the relatively lower boiling temperature of toluene, we used a high-boiling-temperature non-halogenated solvent additive of NMP. The higher boiling point of the additive is beneficial to the appropriate aggregation and self-organization of P3HT and ICBA to obtain the preferred interpenetrating network morphology for high-performance PSCs. Figure 3a shows the *J*−*V* curves of the PSCs based on P3HT/ICBA (1:1, w/w) using toluene as the solvent with NMP additive, and Table 2 summarizes the photovoltaic performance data of the corresponding devices. Interestingly, with 1 vol % NMP additive, PCE of the PSCs based on P3HT/ICBA reached 6.6%, with a V_{oc} of 0.85 V, a J_{sc} of 10.3 mA/cm^2, and a high FF of 75%. The J_{sc} and FF increased greatly for the devices with the NMP additive. However, when the NMP concentration increased to 2%, the PCE of the PSCs dropped to 5.2% with a lower J_{sc} of 9.2 mA/cm^2 and a lower FF of 66%. Furthermore, the photovoltaic performance of PSCs based on P3HT/ICBA fabricated using *o*-xylene, *m*-xylene, or *p*-xylene as the solvent with 1% NMP additive was also characterized, as shown in Figure S3 and Table S2 of the Supporting Information. It was found that, although the J_{sc} and PCE of the corresponding devices also increased using NMP as the additive, the maximum PCE was only 5.5%, which is much lower than that of the device fabricated using toluene as the solvent.

Figure 3b shows the EQE curves of the PSCs based on P3HT/ICBA fabricated using toluene as the solvent with NMP as the additive. The J_{sc} values integrated from the EQE spectra (see Table 2) also agree very well with those measured from the corresponding PSCs. The maximum EQE value of the PSC without NMP additive was 50%, which increased to 65% and 57% after adding 1% and 2% NMP, respectively.

For comparison, we also used NMP additive in fabricating the PSCs based on P3HT/PCBM. Figure S1 of the Supporting Information shows the *J*−*V* curves of the PSCs based on P3HT/PCBM (1:1, w/w) using toluene as the solvent with NMP additive, and Table S1 of the Supporting Information summarizes the photovoltaic performance data of the corresponding devices. It can be seen that adding NMP additive can also improve PCE of the PSCs based on P3HT/PCBM for some extent.

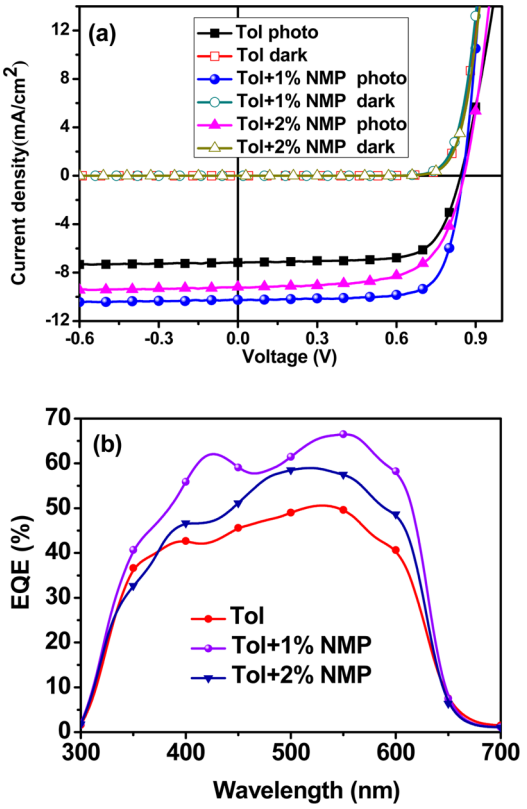

Figure 3. (a) *J*−*V* curves of the PSCs based on P3HT/ICBA (1:1, w/w) processed with toluene solvent with and without NMP additive. (b) EQE curves of the corresponding devices.

Effect of the NMP Additive on the Active-Layer Morphology. We investigated the morphology of the P3HT/ICBA blend active layers by atomic force microscopy (AFM), to understand the effect of the NMP additive on the photovoltaic performance of the PSCs. Figure 4 shows the AFM images of the P3HT/ICBA blend films (1:1, w/w) processed with toluene solvent with or without NMP additive and with pre-thermal annealing at 150 °C for 10 min. It can be seen that, with 1% NMP additive, the blend film demonstrated more uniform morphology and better donor/acceptor interpenetrating network than that of the film without NMP additive. In comparison of the AFM height images (see panels a, c, and e of Figure 4), it can be seen that the surface of the blend films processed with the NMP additive became rougher than that of the film without using the solvent additive, and the roughness increased with the increase of the NMP concentration from 1 to 2%. From the phase images of the blend films in panels b, d, and f of Figure 4, the ordered domains of the

dx.doi.org/10.1021/am500836u | ACS Appl. Mater. Interfaces 2014, 6, 8190−8198

Table 2. Photovoltaic Results of the PSCs Based on P3HT/ICBA (1:1, w/w) Processed with Toluene Solvent with or without NMP Additive under the Illumination of AM 1.5G, 100 mW cm^{-2}

processing solvent	V_{oc} (V)	J_{sc}[a] (mA/cm^2)	FF (%)	PCE best (%)	PCE average[b] (%)
toluene	0.84 ± 0.03	7.2 ± 0.2 (7.2)	71 ± 1	4.5	4.4
toluene + 1% NMP	0.85 ± 0.03	10.3 ± 0.2 (9.9)	75 ± 1	6.6	6.4
toluene + 2% NMP	0.85 ± 0.03	9.2 ± 0.2 (8.9)	66 ± 1	5.2	5.1

[a]The values in parentheses are the J_{sc} calculated from EQE spectra. [b]The average PCE obtained from 20 devices.

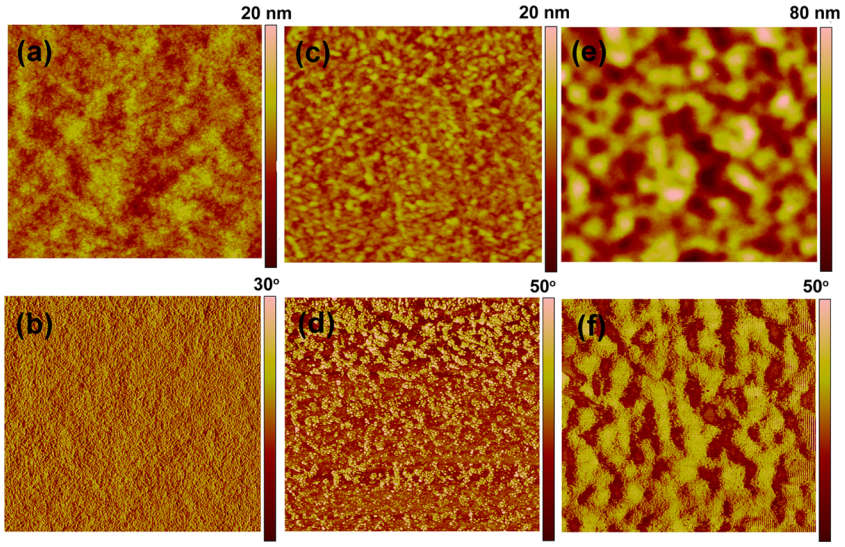

Figure 4. (a, c, and e) AFM (5 × 5 μm) topography and (b, d, and f) phase images of P3HT/ICBA blend films (1:1, w/w) processed with toluene solvent: (a and b) without additive, (c and d) with 1% NMP additive, (e and f) with 2% NMP additive.

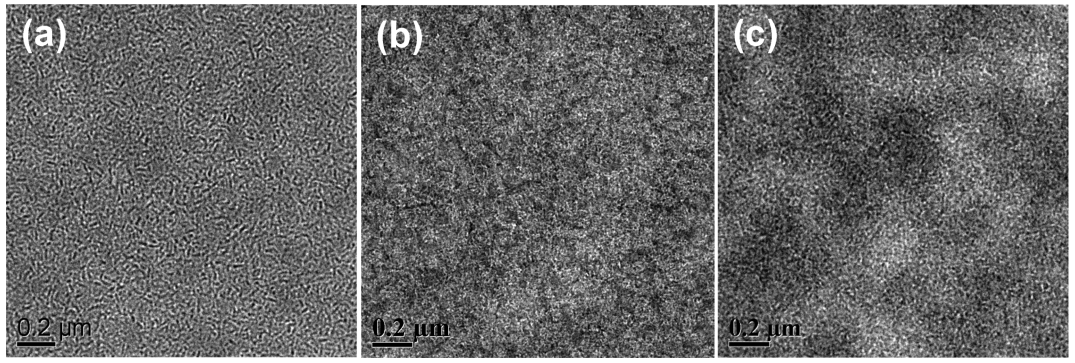

Figure 5. TEM images of the P3HT/ICBA (1:1, w/w) blend films processed with toluene solvent: (a) without additive, (b) with 1% NMP additive, and (c) with 2% NMP additive.

donor and acceptor were improved with the 1% NMP additive in comparison to that without additive, but the domain sizes became too big when the concentration of the NMP additive increased to 2%. The results indicate that the ordered chain alignment is achieved when using NMP as the solvent additive. Obviously, the improvement of the device performance with 1% NMP additive should be beneficial from the improved donor/acceptor interpenetrating network of the blend layer with the additive. However, the domain sizes of the blend layers are too large with 2% NMP additive to decrease the photovoltaic performance. These results indicate that morphology control using an appropriate amount of additive is an effective approach to improve the photovoltaic performance of PSCs.

Actually, the AFM measurement can only observe surface morphology of the blend active layer, while transmission electron microscopy (TEM) can be used to probe the inner-phase-separated morphology of the film. Figure 5 shows the TEM images of the P3HT/ICBA blends processed using toluene as the solvent with or without NMP additive and with pre-thermal annealing at 150 °C for 10 min. The TEM images correlate well with the morphologies observed from AFM. The most significant feature of the films with NMP additive in comparison to that without the additive is the high-contrast dark clusters in the film. The dark clusters in the TEM images should be the ICBA-rich domains reported by Yang et al.[35] Obviously, the NMP additive resulted in the appropriate aggregation of the fullerene acceptors, which improved the photovoltaic performance of the PSCs. The results agree with the literature reports that the solvent additive helps to increase the fullerene domain sizes[39−42] and enlarges the nanoscaled phase separation of the blend films in comparison to that

without using the additive. From the TEM image of the blend film with 1% NMP additive, evident polymer fibrils can be observed in the donor/acceptor interpenetrating networks of the film, which is beneficial to the charge separation and transportation,[42−45] to obtain higher J_{sc} and FF. However, with 2% NMP additive, the aggregation sizes of the polymer donor and fullerene acceptor are too big for efficient exciton charge dissociation; therefore, the photovoltaic performance was decreased.

To fully understand the effect of the additives on the interpenetrating networks of the P3HT/ICBA (1:1, w/w) active layers, we measured X-ray diffraction (XRD) patterns of the active layers. Figure 6 shows the XRD patterns of the active

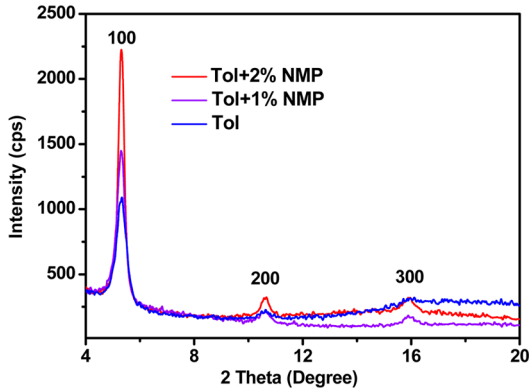

Figure 6. XRD patterns of the P3HT/ICBA (1:1, w/w) blend films prepared with the toluene solvent and with or without the NMP additive.

layers prepared with toluene solvent with or without NMP additive. The XRD pattern exhibits three diffraction peaks at 2θ = 5.32°, 10.64°, and 15.89°, which are the (100), (200), and (300) diffraction peaks of P3HT, respectively. Obviously, the treatment with NMP additive results in an increase of the XRD peak intensity of the blend films; especially, the peak at 2θ = 5.32° (corresponding to the interlayer spacing of ordered P3HT aggregations) is enhanced significantly by the treatment of the NMP additive. The stronger XRD peak indicates the increased crystallinity (or ordered structure) of P3HT aggregation in the blend films with NMP additive. The results confirm that the NMP additive treatment improved the nanoscaled aggregation morphology of the donor and acceptor materials, which agrees very well with the morphologies observed from the AFM and TEM images.

To understand further the origin of the increased photovoltaic performance of the PSCs with the NMP additive, we measured the absorption spectra of P3HT/ICBA (1:1, w/w) blend films processed under the same conditions (thermal annealing at 150 °C for 10 min) with the device fabrication, as shown in Figure 7. We can see that, when using NMP as the additive, the absorbance of the blend films significantly enhanced, which should be attributed to the aggregation of ICBA and the increased crystallinity of P3HT, which have been proven in the above morphological studies and XRD characterization. The stronger absorption of the blend films with the treatment of the NMP additive should be beneficial to the increase of J_{sc} and EQE values for the PSCs with the NMP additive.

The charge carrier mobility was measured by the space charge limited current (SCLC) method.[46] The hole mobility

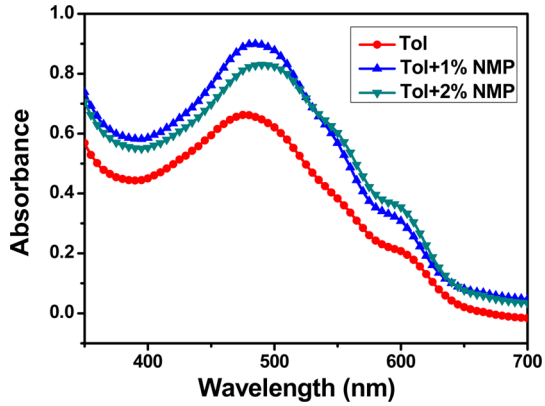

Figure 7. Absorption spectra of the blend films of P3HT/ICBA (1:1, w/w) prepared from toluene solution with or without the NMP additive after thermal annealing at 150 °C for 10 min.

was measured with a hole-only device of ITO/PEDOT:PSS/active layer/Au and estimated by the equation $J \cong (9/8)\varepsilon\varepsilon_0\mu V^2 \exp(0.89(V/E_0L)^{1/2})/L^3$.[47] The electron mobility was measured with an electron-only device of ITO/Al/active layer/Al and estimated by the equation $J = (8/9)\varepsilon_r\varepsilon_0\mu_e(V^2/L^3)$.[48] Figure 8 shows the $J-V$ curves and the plots calculated from $J-V$ curves of different blend films. The detailed hole and the electron mobilities (μ_h and μ_e) are listed in Table 3. Because a PSC device should keep the electric neutrality during the whole photoelectric conversion process, the carrier transport ability should be determined by the "bucket effect"; that is, carrier transport capability of the BHJ blend is determined by the lower one of μ_h and μ_e. According to the mobility results shown in Table 3, we can see that 1% NMP can improve both the μ_h and μ_e, while when the additive content increased to 2%, the μ_h improved a lot but the μ_e decreased. The μ_e values of these four devices can be arranged by the order of $\mu_{e,1\%\ NMP} > \mu_{e,without} > \mu_{e,2\%\ NMP}$, while the μ_h values of these four devices can be arranged by the order of $\mu_{h,2\%\ NMP} > \mu_{h,1\%\ NMP} > \mu_{h,without}$. Because the balanced μ_h and μ_e in the BHJ blend is the key to realize good FF,[49] 1% NMP additive treatment results in the most balanced μ_h and μ_e, so that the higher FF value of the corresponding PSCs was obtained.

From the results mentioned above, we can see that the treatment of 1% NMP additive improved the morphology and interpenetrating network of the active blend layer of the P3HT donor and ICBA acceptor. Actually, the mechanism of adding additive to improve the photovoltaic performance of the PSCs has been well-studied in the literature.[20,39,40] It is well-recognized that the higher boiling point than the processing solvent and selective solubility of the additive for the polymer donor and fullerene derivative acceptor in the active layer play key roles in improving the morphology. To understand further the effect of the NMP additive on the photovoltaic performance of the PSCs based on P3HT/ICBA, we measured the solubility of P3HT and ICBA in toluene and in NMP. P3HT is not soluble in NMP, but ICBA shows excellent solubility of 137.6 mg/mL in NMP, as shown in Table S3 of the Supporting Information. The boiling point of NMP is 202 °C, while that of toluene is 110.6 °C, as also shown in Table S3 of the Supporting Information. Obviously, NMP also shows the selective solubility for the acceptor ICBA and a higher boiling point than toluene, which should be the reason for the improvement of morphology of the active layer of P3HT/ICBA

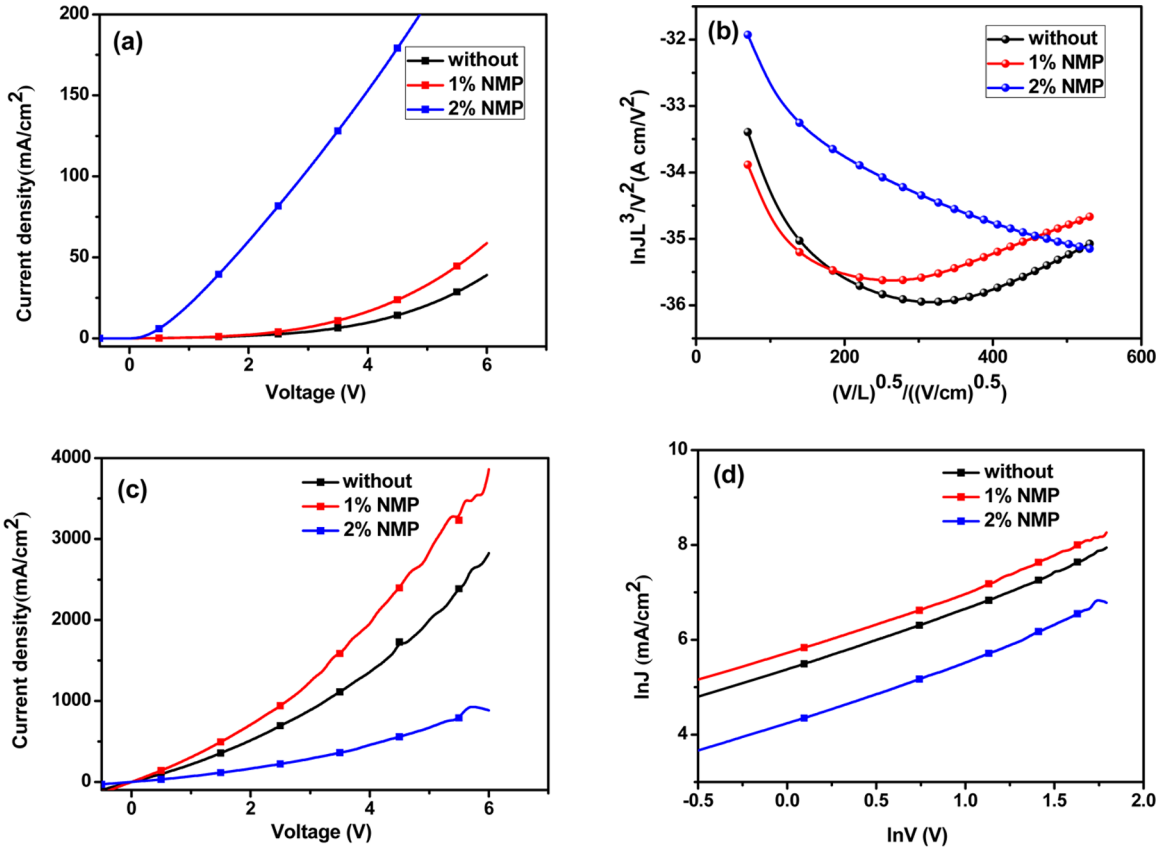

Figure 8. *J*–*V* characteristics of the (a) hole-only and (c) electron-only diodes and corresponding fits to the SCLC model of the (b) hole-only and (d) electron-only diodes of P3HT/ICBA blend films (1:1, w/w) with or without additives.

Table 3. Mobilities of the Blend Films of P3HT/ICBA (1:1, w/w) with or without Additives

additive	μ_h (cm^2 V^{-1} s^{-1})	μ_e (cm^2 V^{-1} s^{-1})	FF (%)
without	1.6×10^{-4}	3.1×10^{-4}	71 ± 1
1% NMP	3.8×10^{-4}	4.5×10^{-4}	75 ± 1
2% NMP	1.3×10^{-2}	9.9×10^{-5}	66 ± 1

prepared from toluene solution with NMP additive than that without the NMP additive.

CONCLUSION

To replace toxic halogenated solvents commonly used in the fabrication of PSCs, we used four non-halogenated solvents of toluene, *o*-xylene, *m*-xylene, and *p*-xylene to fabricate PSCs based on P3HT as the donor and ICBA as the acceptor and compared to the commonly used halogenated solvent *o*-DCB. The PSCs based on P3HT/ICBA (1:1, w/w) with toluene as the solvent and with thermal annealing at 150 °C for 10 min exhibited the optimized performance, with a V_{oc} of 0.84 V, a J_{sc} of 7.2 mA/cm^2, and a FF of 71%, resulting in a PCE of 4.5%, under the illumination of AM 1.5G at 100 mW/cm^2. Then, using 1% NMP solvent additive, the PSCs demonstrated an improved PCE of 6.6%, with a V_{oc} of 0.85 V, a J_{sc} of 10.3 mA/cm^2, and a FF of 75%. We measured AFM and TEM images, XRD patterns, and ultraviolet–visible (UV–vis) absorption spectra of the blend films to investigate the influence of the NMP additive. The results indicate that, with the treatment of 1% NMP additive, the aggregation and crystallinity of P3HT increased and the nanoscaled interpenetrating network of P3HT/ICBA was improved, which are beneficial for the improvement of J_{sc} and PCE. The fabrication of high-performance PSCs with the non-halogenated solvent will play an important role in promoting the commercial application of PSCs.

EXPERIMENTAL SECTION

Materials. P3HT (4002-E) was purchased from Rieke Metals, Inc. and used as received. ICBA was synthesized in our laboratory according to the procedure reported in our previous paper.[17] The ultradry solvents used in fabricating PSCs were bought from Alfa Aesar. PEDOT:PSS (Clevious P VP AI 4083) was obtained fron H. C. Stark, Germany.

Solubility Measurement. Solubilities of ICBA and PCBM in toluene solvent were measured by a standard calibration curve method. First, the absorbance of different concentrations (0.01, 0.02, 0.025, 0.04, and 0.05 mg/mL) of ICBA and PCBM solutions were measured separately to make the standard calibration curves, as shown in Figure 1. Second, ICBA or PCBM powder was added to the toluene solvent to make saturated solutions and centrifuged at 13 500 rpm for 15 min. Then, the top clear solutions in the centrifuge tubes were filtered through a 0.25 μm filter and diluted to measure their absorbance. The solubility values were calculated on the basis of the absorbance values and the working curves.

Device Fabrication and Characterizations. PSC devices with the structure of ITO/PEDOT:PSS/P3HT/ICBA (1:1, w/w)/Ca/Al were fabricated under conditions as follows. A blend solution of P3HT and ICBA was prepared in different solvents at a concentration of 17 mg/mL (P3HT/solvent) and stirred for 5 h at room temperature for complete dissolution. The treatment of ITO-coated glass substrate and its modification with the PEDOT:PSS layer is the same with that reported in ref 20. The P3HT/ICBA blend solution was spin-coated at 800 rpm on the ITO/PEDOT:PSS electrode in a nitrogen glovebox, and then the active layers were thermal-annealed at 150 °C for 10 min.

The devices were completed by evaporating a Ca (20 nm)/Al (80 nm) negative electrode by mask. The thickness was measured by the Bruker Dektak XT profilometer. The current density−voltage (J−V) curves were measured in a N_2 atmosphere using an AM 1.5G solar simulator with an irradiation intensity of 100 mW/cm^2. The EQE was measured by a solar cell spectral response measurement system QE-R3011 (Enli Technology Co., Ltd.). The light intensity at each wavelength was calibrated with a standard single-crystal Si photovoltaic cell.

Absorption spectra were measured on a Hitachi U-3010 UV−vis spectrophotometer. The P3HT/ICBA (1:1, w/w) blend films from different solvents for the UV−vis absorption measurements were prepared on quartz glass substrates. The AFM measurement of the surface morphology of samples was performed on a NanoScope III (Digital Instruments, Tonawanda, NY) in contacting mode with a 5 μm scanner. The P3HT/ICBA (1:1, w/w) blend films on ITO/PEDOT:PSS substrates prepared by the same method as that for device fabrication were used for the AFM measurements. TEM was conducted on a JEOL 2200FS instrument at 200 kV accelerating voltage. In the preparation of the samples for the TEM measurements, the thin active layers (about 100 nm) were prepared by spin coating the donor/acceptor blend solution on ITO/PEDOT:PSS substrates and then thermal annealing at 150 °C for 10 min. The ITO glass with the active layers was submerged in deionized water for ca. 10 min to make the active layers float on the surface of the water. Then, the floating films were picked up on 200-mesh copper grids, which were used as the active-layer samples for the TEM measurement. The XRD patterns of the blend films were measured by a Bruker D8 ADVANCE with Cu Kα (λ = 1.5406 Å) operating on active-layer (about 300 nm) films spin cast on the SiO_2 surface, which is treated with octadecyltrichlorosilane (OTS). A blend film was spin-cast on top of the OTS-treated SiO_2 substrate. Then, the active layer was heated at 150 °C for 10 min.

■ ASSOCIATED CONTENT

Supporting Information

J−V curves of the PSCs based on P3HT/PCBM (1:1, w/w) processed with toluene solvent with and without NMP additive (Figure S1) and those of the PSCs based on P3HT/ICBA processed with *o*-xylene, *m*-xylene, or *p*-xylene with 1% NMP (Figure S3), AFM images of P3HT/ICBA blend films processed with different solvents (Figure S2), photovoltaic results of the PSCs based on P3HT/PCBM (1:1, w/w) processed with toluene solvent with or without NMP additive (Table S1) and those of the PSCs based on P3HT/ICBA processed with *o*-xylene, *m*-xylene, or *p*-xylene with 1% NMP additive (Table S2), and solubilities of P3HT and ICBA in different solvents and the boiling point of different solvents (Table S3). This material is available free of charge via the Internet at http://pubs.acs.org.

■ AUTHOR INFORMATION

Corresponding Authors

*E-mail: zmj2008@iccas.ac.cn.
*E-mail: hjhzlz@iccas.ac.cn.
*E-mail: liyf@iccas.ac.cn.

Notes

The authors declare no competing financial interest.

■ ACKNOWLEDGMENTS

This work was supported by the Ministry of Science and Technology of China (2014CB643501 and 2011AA050523) and the National Natural Science Foundation of China (NSFC) (91333204 and 51203168).

■ REFERENCES

(1) Cheng, Y. J.; Yang, S.; Hsu, C. H. Synthesis of conjugated polymers for organic solar cell applications. *Chem. Rev.* **2009**, *109*, 5868−5923.
(2) Chen, J. W.; Cao, Y. Development of novel conjugated donor polymers for high-efficiency bulk-heterojunction photovoltaic devices. *Acc. Chem. Res.* **2009**, *42*, 1709−1718.
(3) Li, G.; Zhu, R.; Yang, Y. Polymer solar cells. *Nat. Photonics* **2012**, *6*, 153−161.
(4) Li, Y. F. Molecular design of photovoltaic materials for polymer solar cells: Toward suitable electronic energy levels and broad absorption. *Acc. Chem. Res.* **2012**, *45*, 723−733.
(5) Dou, L. T.; You, J. B.; Hong, Z. R.; Xu, Z.; Li, G.; Street, R. A.; Yang, Y. 25th anniversary article: A decade of organic/polymeric photovoltaic research. *Adv. Mater.* **2013**, *25*, 6642−6671.
(6) Guo, X.; Zhang, M. J.; Ma, W.; Ye, L.; Zhang, S. Q.; Liu, S. J.; Ade, H.; Huang, F.; Hou, J. H. Enhanced photovoltaic performance by modulating surface composition in bulk heterojunction polymer solar cells based on PBDTTT-C-T/PC_{71}BM. *Adv. Mater.* **2014**, DOI: 10.1002/adma.201400411.
(7) Liao, S.-H.; Jhuo, H.-J.; Cheng, Y.-S.; Chen, S.-A. Fullerene derivative-doped zinc oxide nanofilm as the cathode of inverted polymer solar cells with low-bandgap polymer (PTB7-Th) for high performance. *Adv. Mater.* **2013**, *25*, 4766−4771.
(8) Zhang, M. J.; Guo, X.; Zhang, S.; Hou, J. Synergistic effect of fluorination on molecular energy level modulation in highly efficient photovoltaic polymers. *Adv. Mater.* **2014**, *26*, 1118−1123.
(9) Zhang, M. J.; Gu, Y.; Guo, X.; Liu, F.; Zhang, S. Q.; Huo, L. J.; Russell, T. P.; Hou, J. H. Efficient polymer solar cells based on benzothiadiazole and alkylphenyl substituted benzodithiophene with a power conversion efficiency over 8%. *Adv. Mater.* **2013**, *25*, 4944−4949.
(10) Zhang, M. J.; Guo, X.; Ma, W.; Zhang, S. Q.; Huo, L. J.; Ade, H.; Hou, J. H. An easy and effective method to modulate molecular energy level of the polymer based on benzodithiophene for the application in polymer solar cells. *Adv. Mater.* **2014**, *26*, 2089−2095.
(11) Zhang, M. J.; Guo, X.; Li, Y. F. Synthesis and characterization of a copolymer based on thiazolothiazole and dithienosilole for polymer solar cells. *Adv. Energy Mater.* **2011**, *1*, 557−560.
(12) Ma, W. L.; Yang, C.; Gong, X.; Lee, K.; Heeger, A. J. Thermally stable, efficient polymer solar cells with nanoscale control of the interpenetrating network morphology. *Adv. Funct. Mater.* **2005**, *15*, 1617−1622.
(13) Li, G.; Shrotriya, V.; Huang, J.; Yao, Y.; Moriarty, T.; Emery, K.; Yang, Y. High-efficiency solution processable polymer photovoltaic cells by self-organization of polymer blends. *Nat. Mater.* **2005**, *4*, 864−868.
(14) He, Y. J.; Li, Y. F. Fullerene derivative acceptors for high performance polymer solar cells. *Phys. Chem. Chem. Phys.* **2011**, *13*, 1970−1983.
(15) Li, C.-Z.; Yip, H.-L.; Jen, A. K.-Y. Functional fullerenes for organic photovoltaics. *J. Mater. Chem.* **2012**, *22*, 4161−4177.
(16) Li, Y. F. Fullerene-bisadduct acceptors for polymer solar cells. *Chem.—Asian J.* **2013**, *8*, 2316−2328.
(17) He, Y. J.; Chen, H. Y.; Hou, J. H.; Li, Y. F. Indene−C_{60} bisadduct: A new acceptor for high-performance polymer solar cells. *J. Am. Chem. Soc.* **2010**, *132*, 1377−1382.
(18) Zhao, G. J.; He, Y. J.; Li, Y. F. 6.5% efficiency of polymer solar cells based on poly(3-hexylthiophene) and indene−C_{60} bisadduct by device optimization. *Adv. Mater.* **2010**, *22*, 4355−4358.
(19) He, Y. J.; Zhao, G. J.; Peng, B.; Li, Y. F. High-yield synthesis and electrochemical and photovoltaic properties of indene−C_{70} bisadduct. *Adv. Funct. Mater.* **2010**, *20*, 3383−3389.
(20) Guo, X.; Cui, C. H.; Zhang, M. J.; Huo, L. J.; Huang, Y.; Hou, J. H.; Li, Y. F. High efficiency polymer solar cells based on poly(3-hexylthiophene)/indene−C_{70} bisadduct with solvent additive. *Energy Environ. Sci.* **2012**, *5*, 7943−7949.
(21) Meng, X. Y.; Zhang, W. Q.; Tan, Z. A.; Du, C.; Li, X. H.; Bo, Z. S.; Li, Y. F.; Wang, T. S.; Jiang, L.; Shu, C. Y.; Wang, C. R.

Dihydronaphthyl-based [60]fullerene bisadducts for efficient and stable polymer solar cells. *Chem. Commun.* **2012**, *48*, 425−427.
(22) Kim, K.-H.; Kang, H.; Nam, S. Y.; Jung, J.; Kim, P. S.; Cho, C.-H.; Lee, C.; Yoon, S. C.; Kim, B. J. Facile synthesis of *o*-xylenyl fullerene multiadducts for high open circuit voltage and efficient polymer solar cells. *Chem. Mater.* **2011**, *23*, 5090−5095.
(23) Voroshazi, E.; Vasseur, K.; Aernouts, T.; Heremans, P.; Baumann, A.; Deibel, C.; Xue, X.; Herring, A. J.; Athans, A. J.; Lada, T. A.; Richter, H.; Rand, B. P. Novel bis-C_{60} derivative compared to other fullerene bis-adducts in high efficiency polymer photovoltaic cells. *J. Mater. Chem.* **2011**, *21*, 17345−17352.
(24) Cheng, Y.-J.; Liao, M.-H.; Chang, C.-Y.; Kao, W.-S.; Wu, C.-E.; Hsu, C.-S. Di(4-methylphenyl)methano-C_{60} bisadduct for efficient and stable organic photovoltaics with enhanced open-circuit voltage. *Chem. Mater.* **2011**, *23*, 4056−4062.
(25) Ye, G.; Chen, S.; Xiao, Z.; Zuo, Q. Q.; Wei, Q.; Ding, L. M. *o*-Quinodimethane-methano[60]fullerene and thieno-*o*-quinodimethanemethano [60]fullerene as efficient acceptor materials for polymer solar cells. *J. Mater. Chem.* **2012**, *22*, 22374−22377.
(26) Faist, M. A.; Shoaee, S.; Tuladhar, S.; Dibb, G. F. A.; Foster, S.; Gong, W.; Kirchartz, T.; Bradley, D. D. C.; Durrant, J. R.; Nelson, J. Understanding the reduced efficiencies of organic solar cells employing fullerene multiadducts as acceptors. *Adv. Energy Mater.* **2013**, *3*, 744−752.
(27) Shoaee, S.; Subramaniyan, S.; Xin, H.; Keiderling, C.; Tuladhar, P. S.; Jamieson, F.; Jenekhe, S. A.; Durrant, J. R. Charge photogeneration for a series of thiazolo-thiazole donor polymers blended with the fullerene electron acceptors PCBM and ICBA. *Adv. Funct. Mater.* **2013**, *23*, 3286−3298.
(28) Bronstein, H.; Hurhangee, M.; Fregoso, E. C.; Beatrup, D.; Soon, Y. W.; Huang, Z.; Hadipour, A.; Tuladhar, P. S.; Rossbauer, S.; Sohn, E. H.; Shoaee, S.; Dimitrov, S. D.; Frost, J. M.; Ashraf, R. S.; Kirchartz, T.; Watkins, S. E.; Song, K.; Anthopoulos, T.; Nelson, J.; Rand, B. P.; Durrant, J. R.; McCulloch, I. Isostructural, deeper highest occupied molecular orbital analogues of poly(3-hexylthiophene) for high-open circuit voltage organic solar cells. *Chem. Mater.* **2013**, *25*, 4239−4249.
(29) Acton, D. W.; Barker, J. F. In-situ biodegradation potential of aromatic hydrocarbons in anaerobic groundwaters. *J. Contam. Hydrol.* **1992**, *9*, 325−352.
(30) Yu, G.; Gao, J.; Hummelen, J. C.; Wudl, F.; Heeger, A. J. Polymer photovoltaic cells: enhanced efficiencies via a network of internal donor−acceptor heterojunctions. *Science* **1995**, *270*, 1789−1791.
(31) Shaheen, S. E.; Brabec, C. J.; Sariciftci, N. S.; Padinger, F.; Fromherz, T.; Hummelen, J. C. 2.5% efficient organic plastic solar cells. *Appl. Phys. Lett.* **2001**, *78*, 841−843.
(32) Park, C. D.; Fleetham, T. A.; Li, J.; Vogt, B. D. High performance bulk-heterojunction organic solar cells fabricated with non-halogenated solvent processing. *Org. Electron.* **2011**, *12*, 1465−1470.
(33) Chen, K. S.; Yip, H. L.; Schlenker, C. W.; Ginger, D. S.; Jen, A. K. Y. Halogen-free solvent processing for sustainable development of high efficiency organic solar cells. *Org. Electron.* **2012**, *13*, 2870−2878.
(34) Chueh, C. C.; Yao, K.; Yip, H. L.; Chang, C. Y.; Xu, Y. X.; Chen, K. S.; Li, C. Z.; Liu, P.; Huang, F.; Chen, Y. W.; Chen, W. C.; Jen, A. K. Y. Non-halogenated solvents for environmentally friendly processing of high-performance bulk-heterojunction polymer solar cells. *Energy Environ. Sci.* **2013**, *6*, 3241−3248.
(35) Yang, X. N.; Loos, J.; Veenstra, S. C.; Verhees, W. J. H.; Wienk, M. M.; Kroon, J. M.; Michels, M. A. J.; Janssen, R. A. J. Nanoscale morphology of high-performance polymer solar cells. *Nano Lett.* **2005**, *5*, 579−583.
(36) Troshin, P. A.; Hoppe, H.; Renz, J.; Egginger, M.; Mayorova, J. Y.; Goryachev, A. E.; Peregudov, A. S.; Lyubovskaya, R. N.; Gobsch, G.; Sariciftci, N. S.; Razumov, V. F. Material solubility−photovoltaic performance relationship in the design of novel fullerene derivatives for bulk heterojunction solar cells. *Adv. Funct. Mater.* **2009**, *19*, 779−788.
(37) Ruoff, R. S.; Tse, D. S.; Malhotra, R.; Lorents, D. C. Solubility of Ca in a variety of solvents. *J. Phys. Chem.* **1993**, *97*, 3379−3383.
(38) Matsuo, Y.; Kawai, J.; Inada, H.; Nakagawa, T.; Ota, H.; Otsubo, S.; Nakamura, E. Addition of dihydromethano group to fullerenes to improve the performance of bulk heterojunction organic solar cells. *Adv. Mater.* **2013**, *43*, 6266−6269.
(39) Lee, J. K.; Ma, W. L.; Brabec, C. J.; Yuen, J.; Moon, J. S.; Kim, J. Y.; Lee, K.; Bazan, G. C.; Heeger, A. J. Processing additives for improved efficiency from bulk heterojunction solar cells. *J. Am. Chem. Soc.* **2008**, *130*, 3619−3623.
(40) Guo, X.; Zhang, M. J.; Huo, L. J.; Cui, C. H.; Wu, Y.; Hou, J. H.; Li, Y. F. Poly(thieno[3,2-*b*]thiophene-*alt*-bithiazole): A D−A copolymer donor showing improved photovoltaic performance with indene−C_{60} bisadduct acceptor. *Macromolecules* **2012**, *45*, 6930−6937.
(41) Ren, G. Q.; Ahmed, E.; Jenekhe, S. A. Non-fullerene acceptor-based bulk heterojunction polymer solar cells: Engineering the nanomorphology via processing additives. *Adv. Energy Mater.* **2011**, *1*, 946−953.
(42) Nuzzo, D. D.; Aguirre, A.; Shahid, M.; Gevaerts, V. S.; Meskers, S. C.; Janssen, R. A. J. Improved film morphology reduces charge carrier recombination into the triplet excited state in a small bandgap polymer-fullerene photovoltaic cell. *Adv. Mater.* **2010**, *22*, 4321−4324.
(43) Zhang, M. J.; Fan, H. J.; Guo, X.; He, Y. J.; Zhang, Z. G.; Min, J.; Zhang, J.; Zhao, G. J.; Zhan, X. W.; Li, Y. F. Synthesis and photovoltaic properties of bithiazole-based donor−acceptor copolymers. *Macromolecules* **2010**, *43*, 5706−5712.
(44) Zhang, M. J.; Guo, X.; Wang, X. C.; Wang, H. Q.; Li, Y. F. Synthesis and photovoltaic properties of D−A copolymers based on alkyl-substituted indacenodithiophene donor unit. *Chem. Mater.* **2011**, *23*, 4264−4270.
(45) Gu, Y.; Wang, C.; Russell, T. P. Multi-length-scale morphologies in PCPDTBT/PCBM bulk-heterojunction solar cells. *Adv. Energy Mater.* **2012**, *2*, 683−690.
(46) Malliaras, G. G.; Salem, J. R.; Brock, P. J.; Scott, C. Electrical characteristics and efficiency of single-layer organic light-emitting diodes. *Phys. Rev. B: Condens. Matter Mater. Phys.* **1998**, *58*, 13411−13414.
(47) Zhang, M. J.; Guo, X.; Zhang, Z.-G.; Li, Y. F. D−A copolymers based on dithienosilole and phthalimide for photovoltaic materials. *Polymer* **2011**, *52*, 5464−5470.
(48) Zhao, G. J.; He, Y. J.; Xu, Z.; Hou, J. H.; Zhang, M. J.; Min, J.; Chen, H.-Y.; Ye, M. F.; Hong, Z. R.; Yang, Y.; Li, Y. F. Effect of carbon chain length in the substituent of PCBM-like molecules on their photovoltaic properties. *Adv. Funct. Mater.* **2010**, *20*, 1480−1487.
(49) Guo, X.; Zhang, M. J.; Tan, J. H.; Zhang, S. Q.; Huo, L. J.; Hu, W. P.; Li, Y. F.; Hou, J. H. Influence of D/A ratio on photovoltaic performance of a highly efficient polymer solar cell system. *Adv. Mater.* **2012**, *24*, 6536−6541.